COMMUNICATIONS IN COMPUTATIONAL PHYSICS
Vol. **4**, No. 4, pp. 929-948

Commun. Comput. Phys.
October 2008

Numerical Study of Heat and Moisture Transfer in Textile Materials by a Finite Volume Method

C. Ye[1], H. Huang[2], J. Fan[3] and W. Sun[1,*]

[1] *Department of Mathematics, City University of Hong Kong, Kowloon, Hong Kong.*
[2] *Department of Mathematics & Statistics, York University, Toronto, Ontario M3J 1P3, Canada.*
[3] *Institute of Textiles and Clothing, Hong Kong Polytechnic University, Hong Kong.*

Received 28 September 2007; Accepted (in revised version) 6 February 2008

Available online 4 June 2008

Abstract. This paper focuses on the numerical study of heat and moisture transfer in clothing assemblies, based on a multi-component and multiphase flow model which includes heat/moisture convection and conduction/diffusion as well as phase change. A splitting semi-implicit finite volume method is proposed for solving a set of nonlinear convection-diffusion-reaction equations, in which the calculation of liquid water content absorbed by fiber is decoupled from the rest of the computation. The method maintains the conservation of air, vapor and heat flux (energy). Four types of clothing assemblies are investigated and comparison with experimental measurements are also presented.

AMS subject classifications: 78M20, 65N22, 65N06

Key words: Fibrous porous medium, multi-component flow, clothing assemblies, finite volume method, condensation/evaporation.

1 Introduction

Heat and mass transfer in fibrous porous media attracts considerable attention since it can be found in a wide range of industrial and engineering domains, such as paper and pulp [7], building materials [1] and more recently, textile [17, 21]. Heat and moisture transfer with phase change is coupled in rather complicated mechanisms. Henry started to investigate the diffusion of moisture into bales of cotton in 1939 [9] and again in 1948 [10]. Later, David and Nordon [2] improved this model by incorporating several features omitted by Henry. Ogniewicz and Tien [19] proposed a quasi-steady state model to

*Corresponding author. *Email addresses:* hhuang@yorku.ca (H. Huang), tcfanjt@inet.polyu.edu.hk (J. Fan), maweiw@math.cityu.edu.hk (W. Sun)

describe heat and mass transfer with immobile condensation in porous insulation (building material). This model was extended by Shapiro and Motakef [20] to analyze unsteady heat and mass transfer. Recently, Fan et al. [3–5] introduced dynamic moisture absorption and radiation heat transfer into the existing models for clothing assemblies. In their model, the mixture velocity is determined by the vapor pressure. A more realistic mathematical model for moisture transport in clothing assemblies was proposed by Huang et al. [11]. Their model is a generalization of a single-component model used in [5] to a multi-component model by treating air and vapor separately.

This paper focuses on the numerical investigation of heat and moisture transfer in clothing assemblies, based mainly on the model proposed in [11] with several further modifications. Since the volume fraction of water is relative small, a simplified water equation is introduced in this paper by neglecting convection and diffusion (capillary effect) for liquid water. Therefore, liquid water is immobile and stays at the condensation site. Heat conductivity depends upon the conductivity of each material in the clothing assemblies and their suitable combination. The effective heat conductivity is obtained by a combination of parallel and serial distributions, depending on the amount of water/ice. The capacity of mixture is treated in the same way. Since the model consists of a system of nonlinear equations, to maintain the conservation of air, vapor and energy, a splitting semi-implicit finite volume method is used. In addition, liquid water content absorbed by fiber is obtained directly from the scaled water content which is computed by solving an evolution equation along the fibre radius with a Dirichlet boundary condition.

The rest of the paper is organized as follows. In Section 2, we introduce the mathematical model of moisture transport in textile materials in a one dimensional setting and a class of physical boundary conditions for a typical clothing assembly, a porous batting sandwiched by two covering layers. The model consists of a system of nonlinear evolution transport equations. In Section 3, we propose a splitting semi-implicit scheme for this system of nonlinear equations using a finite volume method. Numerical results are presented in Section 4. Clothing assemblies with two different batting materials (polyester and viscose) and two different cover materials (nylon and laminated) are investigated numerically by the proposed method and the results are compared with experimental observations [6], which reveal distinct characteristics due to the fact that the two batting materials have different rates of absorption and the two covers have different resistance to air and vapor. Numerical test shows that the proposed method is efficient and numerical results are in better agreement with the experimental data than previous numerical simulations, indicating that the current model is more realistic than the previous ones reported in the literature.

2 Mathematical model

Here we consider a model problem of heat and moisture transfer in textile materials, which consists of a three-layer porous clothing assemblies as illustrated in Fig. 1. The

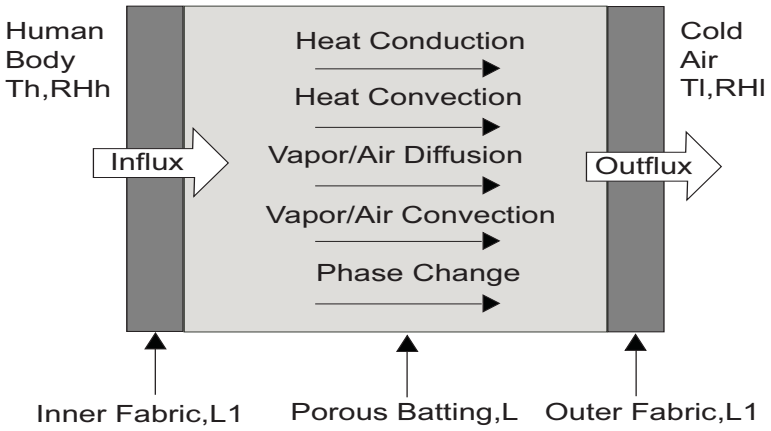

Figure 1: Schematic diagram of the porous clothing assembly.

outside cover of the assembly is exposed to a cold environment with fixed temperature and relative humidity while the inside cover is exposed to a mixture of air and vapor at higher temperature and relative humidity.

From the conservation of mass and energy, the physical process can be described by

$$\frac{\partial}{\partial t}(\epsilon C_v)+\frac{\partial}{\partial x}(u_g\epsilon C_v)=\frac{\partial}{\partial x}\left[\frac{D_g\epsilon}{\tau_c}C\frac{\partial}{\partial x}\left(\frac{C_v}{C}\right)\right]-\Gamma, \tag{2.1}$$

$$\frac{\partial}{\partial t}(\epsilon C_a)+\frac{\partial}{\partial x}(u_g\epsilon C_a)=\frac{\partial}{\partial x}\left[\frac{D_g\epsilon}{\tau_c}C\frac{\partial}{\partial x}\left(\frac{C_a}{C}\right)\right], \tag{2.2}$$

$$\frac{\partial}{\partial t}(C_{vt}T)+\frac{\partial}{\partial x}\left(u_g\epsilon C_{vg}T\right)=\frac{\partial}{\partial x}\left(\kappa\frac{\partial T}{\partial x}\right)+\lambda M\Gamma, \tag{2.3}$$

with a simplified water equation

$$\frac{\partial}{\partial t}\left[\rho(1-\epsilon')\widetilde{W}\right]=M\Gamma_{ce}. \tag{2.4}$$

Here the generalized Fick's law [22] has been used for the binary multi-component gas mixture (vapor and air). C_v, C_a and $C=C_v+C_a$ are the water vapor, air and total (molar) concentrations, $\widetilde{W}$ is the relative liquid water content (%) on the fibre surface, u_g is the molar averaged mixture velocity, τ_c is the tortuosity for the air-vapor diffusion and D_g is the molecular diffusion coefficient for air and vapor. In wet zone, λ is the latent heat of evaporation/condensation while in frozen zone, it represents the latent heat of sublimation. Γ is the (molar) rate of phase change per unit volume and M is the molecular weight of water.

The porosity with liquid water content (ϵ) and without liquid water content (ϵ') are related by

$$\epsilon=\epsilon'-\frac{\rho}{\rho_w}\widetilde{W}(1-\epsilon'). \tag{2.5}$$

The phase change rate Γ consists of two parts, $\Gamma=\Gamma_{ce}+\Gamma_s$, where

$$\Gamma_s=(1-\epsilon')\frac{\partial C_f}{\partial t} \tag{2.6}$$

is the rate due to absorption by the fibre and

$$\Gamma_{ce}=-\frac{E}{R_f}\sqrt{\frac{(1-\epsilon)(1-\epsilon')}{2\pi RM}}\left(\frac{P_{sat}-P_v}{\sqrt{T_s}}\right) \tag{2.7}$$

is the Hertz-Knudsen equation [13] for condensation and evaporation (molar rate), where R is the universal gas constant and R_f is the radius of fibre. The saturation pressure P_{sat} is determined from experimental measurement which is plotted in Fig. 2. The vapor pressure is given by

$$P_v=RC_vT. \tag{2.8}$$

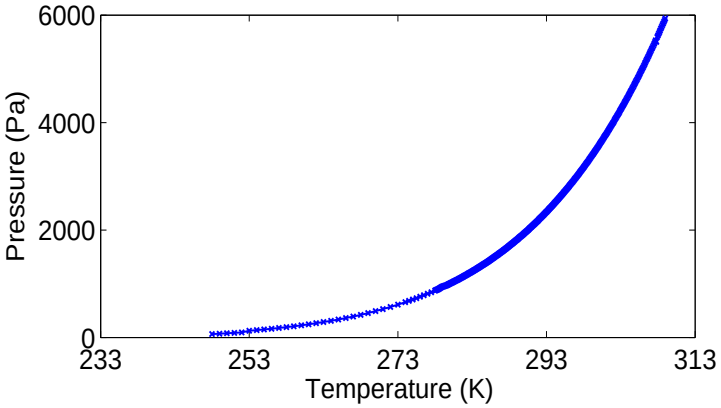

Figure 2: Experimental measurements of saturation pressure.

The amount of water absorbed by fibre C_f (mole per unit volume) in (2.6) is given by

$$C_f=\frac{2}{R_f^2}\int_0^{R_f}C_f'rdr,\qquad \frac{\partial C_f'}{\partial t}=\frac{1}{r}\frac{\partial}{\partial r}\left(D_f r\frac{\partial C_f'}{\partial r}\right),\quad 0\le r\le R_f, t>0 \tag{2.9}$$

with $C_f'(R_f,t)=\rho W_f'(RH)/M$ and $W_f'(RH)$ is available via experimental measurement, *e.g.*, see Fig. 3 for viscose material. Here the relative humidity is defined by $RH=P_v/P_{sat}$ and D_f is the diffusion coefficient of moisture in fiber.

The total heat volumetric water content W (%) is the sum of the water absorbed by the fiber and the water on the fiber surface, *i.e.*,

$$W=\widetilde{W}+W_f,\qquad W_f=\frac{MC_f}{\rho}=\frac{2M}{\rho R_f^2}\int_0^{R_f}C_f'rdr. \tag{2.10}$$

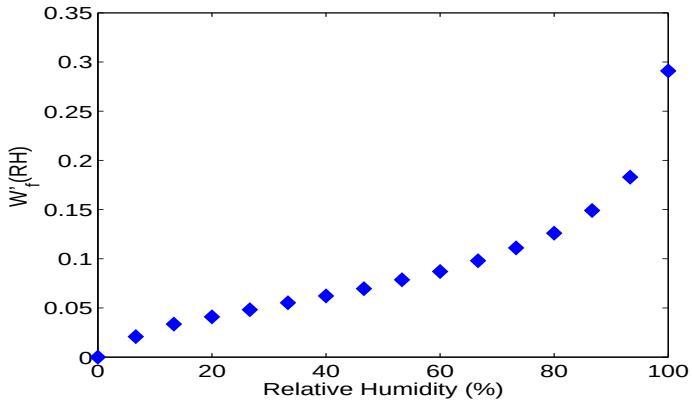

Figure 3: Experimental measurements of the maximum water content absorbed by viscose material (W_f').

The effective heat conductivity for gas-fiber-water mixture depends upon the conductivities of gas, vapor and water/ice. A general form is given by

$$\kappa = \epsilon\kappa_g + (1-\epsilon)\kappa_{f'}, \tag{2.11}$$

where κ_g is the heat conductivity of gas and $\kappa_{f'}$ is the conductivity of fiber-water mixture. In general, either parallel and serial combinations may be used to obtain the effective conductivity. In this paper we use a combined form as

$$\kappa_{f'} = \omega_k \kappa_{f_p'} + (1-\omega_k)\kappa_{f_s'}. \tag{2.12}$$

Here ω_k $(0 \le \omega_k \le 1)$ depends on the amount of water content and $\omega_k = 1$ when the water content is relative small, *i.e.*, the conductivity of the fiber-water mixture is defined in a serial form of fiber and water conductivities. Conductivities in parallel and serial forms are given by

$$\kappa_{f_p'} = \left(\kappa_f + \frac{\rho}{\rho_w} W\kappa_w\right)\left(1+\frac{\rho}{\rho_w}W\right)^{-1} \tag{2.13}$$

and

$$\kappa_{f_s'} = \left(\frac{1}{\rho_f} + \frac{W}{\rho_w}\right)\left(\frac{1}{\rho\kappa_f} + \frac{W}{\rho_w\kappa_w}\right)^{-1}, \tag{2.14}$$

where κ_w and κ_f are the heat conductivity for water and fibre, respectively.

In the same way, the effective volumetric heat capacity can be obtained as

$$\begin{aligned} C_{vt} = \epsilon C_{vg} + (1-\epsilon)\Bigg[&\omega_c\left(C_{vf} + \frac{\rho}{\rho_w}WC_{vw}\right)\left(1+\frac{\rho}{\rho_w}W\right)^{-1} \\ &+ (1-\omega_c)\left(\frac{1}{C_{vf}} + \frac{W}{\rho_w}\right)\left(\frac{1}{\rho C_{vf}} + \frac{W}{\rho_w C_{vw}}\right)^{-1}\Bigg], \end{aligned} \tag{2.15}$$

where C_{vg}, C_{vf} and C_{vw} are the heat capacity for vapor/air, fibre and water, respectively.

The vapor-air mixture velocity (volumetric discharge) is given by the Darcy's law

$$u_g = -\frac{kk_{rg}}{\mu_g}\frac{\partial P_g}{\partial x}, \tag{2.16}$$

where k is the permeability, k_{rg} and μ_g are the relative permeability and the viscosity of the gas mixture, respectively. $P_g = P_v + P_a$ is the total gas pressure. k_{rg} can be obtained by the empirical relations $k_{rg} = (1-s)^3$. Here, s is the volumetric liquid saturation in the inter fibre void space, which is related to the water content by

$$s = \frac{(1-\epsilon')\rho\widetilde{W}}{\epsilon'\rho_w}. \tag{2.17}$$

The solution of the model highly depends on the boundary conditions and developing appropriate initial and boundary conditions is important. Since the cover layers are much thinner than the batting layer, the properties of heat and moisture transfer on the covers may be described by simple resistances to heat, vapor and air transfer. A class of Robin type boundary conditions were introduced in [5] to approximate the experimental setup in [6], in which boundary conditions are defined by a combined simulation of cover layers and ambient environment. These Robin type boundary conditions are used in this paper.

At the inner cover,

$$\begin{aligned}
&u_g\epsilon C_v - \frac{D_g\epsilon}{\tau_c}C\frac{\partial}{\partial x}\left(\frac{C_v}{C}\right)\Big|_{x=0} = \frac{1}{R_v^i + 1/H_v^i}(C_v - C_v^i),\\
&u_g\epsilon C_a - \frac{D_g\epsilon}{\tau_c}C\frac{\partial}{\partial x}\left(\frac{C_a}{C}\right)\Big|_{x=0} = \frac{1}{R_a^i + 1/H_a^i}(C_a - C_a^i),\\
&u_g\epsilon C_{vg}T - \kappa\frac{\partial T}{\partial x}\Big|_{x=0} = \frac{1}{R_t^i + 1/H_t^i}(T - T^i),
\end{aligned}$$

where R_v^i and R_a^i are the resistances of the inner cover to vapor and air, respectively, and R_t^i is the resistance of the inner cover to heat. H_v^i and H_a^i are the mass transfer coefficients of the inner environment for vapor and air, respectively, and H_t^i is the heat transfer coefficient of the inner environment for heat. For vapor, we assume a relative humidity 100% due to a constant evaporation, i.e., $RH^i = 1$. Therefore the vapor concentration can be computed by the following formula

$$C_v^i = RH^i\frac{P_{sat}(T^i)}{RT^i}, \tag{2.18}$$

where T^i is the inner temperature.

We assume that the background air pressure is the atmospheric pressure P_{atm}, from which the air concentration can be calculated by

$$C_a^i = \frac{P_{atm}}{RT^i}. \tag{2.19}$$

Similar to the inner boundary, we have the boundary conditions on the outer boundary

$$u_g\epsilon C_v-\frac{D_g\epsilon}{\tau_c}C\frac{\partial}{\partial x}(\frac{C_v}{C})\Big|_{x=L}=\frac{1}{R_v^o+1/H_v^o}(C_v^o-C_v),$$
$$u_g\epsilon C_a-\frac{D_g\epsilon}{\tau_c}C\frac{\partial}{\partial x}(\frac{C_a}{C})\Big|_{x=L}=\frac{1}{R_a^o+1/H_a^o}(C_a^o-C_a),$$
$$u_g\epsilon C_{vg}T-\kappa\frac{\partial T}{\partial x}\Big|_{x=L}=\frac{1}{R_t^o+1/H_t^o}(T^o-T),$$

where R_v^o,R_a^o, R_t^o, H_v^o, H_a^o, H_v^o and H_t^o are defined analogously. We assume that the background temperature is fixed at T^o (e.g., $-20^\circ C$) with a relative humidity of RH^o (e.g., 90%). The background vapor concentration can be calculated by

$$C_v^o=RH^o\frac{P_{sat}(T^o)}{RT^o}. \tag{2.20}$$

and the air concentration can be obtained by

$$C_a^o=\frac{P_{atm}}{RT^o}. \tag{2.21}$$

The initial conditions at $t=0$ are given by

$$T=25^\circ C,\quad C_v=65\%\frac{P_{sat}(T)}{RT},\quad C_a=\frac{P_{atm}}{RT},\quad \widetilde{W}=0. \tag{2.22}$$

3 Numerical method

In this section, we present a splitting semi-implicit scheme and a finite volume method for Eqs. (2.1)-(2.4), and the calculation for the water absorption by fiber is decoupled. In many practical flow problems, pressure P is often used as a main variable. To obtain an equation for pressure, we add Eqs. (2.1)-(2.2) together and by noting

$$P=RCT,\quad C=C_v+C_a,$$

we have

$$\frac{\partial}{\partial t}\Big(\frac{\epsilon}{RT}P\Big)+\frac{\partial}{\partial x}\Big(u_g\epsilon\frac{P}{RT}\Big)=-\Gamma_{ce}-\Gamma_s. \tag{3.1}$$

Corresponding initial-boundary conditions for the pressure equation can be obtained in the same way,

$$\begin{aligned}&P^0=P_{atm}+65\%P_{sat}(T),\quad t=0,\\ &u_g\epsilon\frac{P}{RT}\Big|_{x=0}=\frac{1}{R_v^i+1/H_v^i}(C_v-C_v^i)+\frac{1}{R_a^i+1/H_a^i}(C_a-C_a^i),\\ &u_g\epsilon\frac{P}{RT}\Big|_{x=L}=\frac{1}{R_v^o+1/H_v^o}(C_v^o-C_v)+\frac{1}{R_a^o+1/H_a^o}(C_a^o-C_a).\end{aligned} \tag{3.2}$$

The discrete system presented in this section is based on approximations to the variables P, T, C_v and $\widetilde{W}$.

3.1 Finite volume discretization with splitting

Let $x_j = j\Delta x$ be a uniform partition in [0,L] and $t_n = n\Delta t$ be a uniform partition for $t>0$, where $\Delta x = L/(N-1)$. Denote by P_j^n, $C_{v,j}^n$, T_j^n and $\widetilde{W}_j^n$ the numerical solutions of pressure, vapor concentration, temperature and water/ice content in $x=x_j$ and $t=t_n$, respectively. Finite volume discretizations can be obtained on the basis of integral form of the flux conservation in the spatial cell $(x_{j-1/2}, x_{j+1/2})$ and the time interval (t_n, t_{n+1}). The detailed derivation for general finite volume methods can be found in [8, 12, 14, 16, 23]. Since the source term is nonlinear for temperature and linear for vapor concentration, we propose a splitting finite volume method in which the discrete water equation is approximated by

$$\frac{\rho(1-\epsilon')}{\Delta t}(\widetilde{W}_j^{n+1}-\widetilde{W}_j^n)=\beta_W S_{1,j}^n, \qquad j=2,\cdots,N-1 \tag{3.3}$$

and discrete equations for other quantities are given by

$$\begin{aligned}\frac{C_{vt,j}^{n+1}T_j^{n+1}-C_{vt,j}^n T_j^n}{\Delta t} &= \frac{V_{T,j}}{\Delta x}\delta_x\left(\epsilon_{j+1/2}^n V_{j+1/2}^n \frac{(T_j^{n+1}+T_{j+1}^{n+1})}{2}\right)\\ &+\frac{1}{(\Delta x)^2}\delta_x\left(\kappa_{j+1/2}^n\delta_x T_{j+1}^{n+1}\right)+\beta_T\left.\frac{\partial S_1}{\partial T}\right|_{T=T_j^n}(T_j^{n+1}-T_j^n)+\beta_T S_{1,j}^n+\lambda M\Gamma_{s,j}^n, \qquad (3.4)\\ \frac{\epsilon_j^{n+1}C_{v,j}^{n+1}-\epsilon_j^n C_{v,j}^n}{\Delta t} &= \frac{V_{G,j}}{(\Delta x)}\delta_x\left(\epsilon_{j+1/2}^n V_{j+1/2}^n\frac{(C_{v,j+1}^{n+1}+C_{v,j}^{n+1})}{2}\right)\\ &+\frac{\delta_G}{(\Delta x)^2}\delta_x\left(\epsilon_{j+1/2}^n C_{j+1/2}^n\delta_x\left(\frac{C_{v,j+1}^{n+1}}{C_{j+1}^n}\right)\right)-\beta_G S_{1,j}^{n+1}-\Gamma_{s,j}^n, \qquad (3.5)\\ \frac{\epsilon_j^{n+1}P_j^{n+1}}{RT_j^{n+1}\Delta t}-\frac{\epsilon_j^n P_j^n}{RT_j^n\Delta t} &= \frac{V_{G,j}}{(\Delta x)^2}\delta_x\left(\frac{\epsilon_{j+1/2}^n P_{j+1/2}^n}{RT_{j+1/2}^n}\delta_x P_{j+1}^{n+1}\right)-\beta_G S_{1,j}^{n+1}-\Gamma_{s,j}^n, \qquad (3.6)\end{aligned}$$

where

$$\begin{aligned}&\delta_x\alpha_j=\alpha_j-\alpha_{j-1}, \quad V_j^n=\frac{1}{\Delta x}\delta_x P_{j+1/2}^n, \quad V_G=\frac{kk_{rg}}{\mu_g}, \quad V_T=\frac{kk_{rg}C_{vg}}{\mu_g},\\ &S_1=\sqrt{1+\frac{\rho}{\rho_w}\widetilde{W}}\left(\frac{C_v RT-P_{sat}}{\sqrt{T}}\right), \quad \delta_G=\frac{D_a}{\tau_c}, \quad \beta_G=\frac{E(1-\epsilon')}{R_f\sqrt{2\pi RM}},\\ &\beta_T=\frac{\lambda E(1-\epsilon')}{R_f}\sqrt{\frac{M}{2\pi R}}, \quad \beta_W=\frac{E(1-\epsilon')}{R_f}\sqrt{\frac{M}{2\pi R}};\end{aligned} \tag{3.7}$$

and $\Gamma_{s,j}^n$ is calculated separately and the details will be presented in the next subsection. Note that the mixture velocity u_g in the convection term is treated explicitly in the vapor and temperature equations, and implicitly in the pressure equation since the convection

term in the latter behaves as a diffusive term. The phase change (source) term in the temperature equation is linearized and treated implicitly.

To derive finite volume type discrete boundary conditions, the integral form of the conservation law is applied in the spatial interval (x_1, $x_{3/2}$) and the time interval (t_n, t_{n+1}). For the pressure equation, we have

$$\begin{aligned}&\int_{x_1}^{x_{3/2}}\int_{t_n}^{t_{n+1}}\frac{\partial}{\partial t}\left(\frac{\epsilon}{RT}P\right)dtdx\\&=\int_{t_n}^{t_{n+1}}\int_{x_1}^{x_{3/2}}\frac{\partial}{\partial x}\left(V_G\epsilon\frac{P}{RT}\frac{\partial P}{\partial x}\right)dxdt-\int_{x_1}^{x_{3/2}}\int_{t_n}^{t_{n+1}}(\beta_G S_1+\Gamma_s)dtdx,\end{aligned}\tag{3.8}$$

which leads to

$$\begin{aligned}&\int_{x_1}^{x_{3/2}}\left[\left(\frac{\epsilon}{RT}P\right)\Big|_{t_{n+1}}-\left(\frac{\epsilon}{RT}P\right)\Big|_{t_n}\right]dx\\&=\int_{t_n}^{t_{n+1}}\left[\left(V_G\epsilon\frac{P}{RT}\frac{\partial P}{\partial x}\right)\Big|_{x_{3/2}}-\left(V_G\epsilon\frac{P}{RT}\frac{\partial P}{\partial x}\right)\Big|_{x_1}\right]dt-\int_{x_1}^{x_{3/2}}\int_{t_n}^{t_{n+1}}(\beta_G S_1+\Gamma_s)dtdx.\end{aligned}\tag{3.9}$$

And furthermore,

$$\begin{aligned}\frac{\Delta x}{2}\left(\frac{\epsilon_1^{n+1}}{RT_1^{n+1}}P_1^{n+1}-\frac{\epsilon_1^n}{RT_1^n}P_1^n\right)&=\Delta tV_G\epsilon_{3/2}^n\frac{P_{3/2}^n}{RT_{3/2}^n}\frac{(P_2^{n+1}-P_1^{n+1})}{\Delta x}\\&\quad-\Delta t\left(V_G\epsilon\frac{P}{RT}\frac{\partial P}{\partial x}\right)\Big|_{x_1,t_{n+1}}-\frac{\Delta x}{2}\Delta t(\beta_G S_{1,1}^{n+1}+\Gamma_{s,1}^n).\end{aligned}\tag{3.10}$$

Replacing the second last term in (3.10) with the boundary condition (3.2), we obtain a finite volume type discrete boundary condition for the pressure equation at the inner boundary

$$\begin{aligned}\frac{\Delta x}{2}\left(\frac{\epsilon_1^{n+1}}{RT_1^{n+1}}P_1^{n+1}-\frac{\epsilon_1^n}{RT_1^n}P_1^n\right)&=\Delta tV_{G,3/2}\epsilon_{3/2}^n\frac{P_{3/2}^n}{RT_{3/2}^n}\frac{(P_2^{n+1}-P_1^{n+1})}{\Delta x}\\&\quad-\Delta t\left(\frac{C_{v,1}^{n+1}-C_v^i}{R_v^i+1/H_v^i}+\frac{C_{a,1}^n-C_a^i}{R_a^i+1/H_a^i}\right)-\frac{\Delta x}{2}\Delta t(\beta_G S_{1,1}^{n+1}+\Gamma_{s,1}^n).\end{aligned}\tag{3.11}$$

The rest of the boundary conditions can be obtained analogously as

$$\widetilde{W}_2^{n+1}-\widetilde{W}_1^{n+1}=0,\tag{3.12}$$

$$\begin{aligned}C_{vt,1}^{n+1}T_1^{n+1}-C_{vt,1}^{n+1}T_1^n&=\frac{2\Delta t}{\Delta x^2}\left[V_{T,3/2}\epsilon_{3/2}^n\delta_xP_2^nT_{3/2}^{n+1}+\kappa_{3/2}^n\delta_xT_2^{n+1}\right]-\frac{2\Delta t}{\Delta x}\frac{T_1^{n+1}-T^i}{R_t^i+1/H_t^i}\\&\quad+\Delta t\beta_T\frac{\partial S_1}{\partial T}\Big|_{T=T_1^n}(T_1^{n+1}-T_1^n)+\Delta t(\beta_T S_{1,1}^n+\lambda M\Gamma_{s,1}^n),\end{aligned}\tag{3.13}$$

$$\epsilon_1^{n+1}C_{v,1}^{n+1}-\epsilon_1^nC_{v,1}^n=\frac{2\Delta t}{\Delta x^2}\left[V_{G,3/2}\delta_xP_2^nC_{v,3/2}^{n+1}+\delta_GC_{3/2}^n\delta_x\left(C_{v,2}^{n+1}/C_2^n\right)\right]\epsilon_{3/2}^n$$
$$-\frac{2\Delta t}{\Delta x}\frac{C_{v,1}^{n+1}-C_v^i}{R_v^i+1/H_v^i}-\Delta t(\beta_GS_{1,1}^{n+1}+\Gamma_{s,1}^n), \tag{3.14}$$

at $x=0$; and

$$\widetilde{W}_N^{n+1}-\widetilde{W}_{N-1}^{n+1}=0, \tag{3.15}$$

$$C_{vt,N}^{n+1}T_N^{n+1}-C_{vt,N}^nT_{N-1}^n=-\frac{2\Delta t}{\Delta x^2}\left[V_{T,N-1/2}\epsilon_{N-1/2}^n\delta_xP_N^nT_{N-1/2}^{n+1}+\kappa_{N-1/2}^n\delta_xT_N^{n+1}\right]$$
$$+\frac{2\Delta t}{\Delta x}\frac{T^o-T_N^{n+1}}{R_t^o+1/H_t^o}+\Delta t\beta_T\left.\frac{\partial S_1}{\partial T}\right|_{T=T_N^n}(T_N^{n+1}-T_N^n)+\Delta t(\beta_TS_{1,N}^n+\lambda M\Gamma_{s,N}^n), \tag{3.16}$$

$$\epsilon_N^{n+1}C_{v,N}^{n+1}-\epsilon_N^nC_{v,N}^n=\frac{2\Delta t}{\Delta x}\frac{C_v^o-C_{v,N}^{n+1}}{R_v^o+1/H_v^o}-\Delta t(\beta_GS_{1,N}^{n+1}+\Gamma_{s,N}^n)$$
$$-\frac{2\Delta t}{\Delta x^2}\left[V_{G,N-1/2}\delta_xP_N^nC_{v,N-1/2}^{n+1}+\delta_GC_{N-1/2}^n\delta_x\left(C_{v,N}^{n+1}/C_N^n\right)\right]\epsilon_{N-1/2}^n, \tag{3.17}$$

$$\frac{\epsilon_N^{n+1}}{RT_N^{n+1}}P_N^{n+1}-\frac{\epsilon_N^n}{RT_N^n}P_N^n=-\frac{2\Delta t}{\Delta x^2}V_{G,N-1/2}\epsilon_{N-1/2}^n\frac{P_{N-1/2}^n}{RT_{N-1/2}^n}\delta_xP_N^{n+1}$$
$$-\Delta t(\beta_GS_{1,N}^{n+1}+\Gamma_{s,N}^n)+\frac{2\Delta t}{\Delta x}\left[\frac{C_v^o-C_{v,N}^{n+1}}{R_v^o+1/H_v^o}+\frac{C_a^o-C_{a,N}^n}{R_a^o+1/H_a^o}\right] \tag{3.18}$$

at $x=1$. The computational procedure of the splitting scheme at each time step is outlined below.

Algorithm 3.1:

(i). The free water content $\widetilde{W}_j^{n+1}$ is first obtained by solving the discrete water equation (3.3). The total water content W^{n+1} is calculated by adding the water content absorbed by fiber W_f^{n+1} (see next section) and $\widetilde{W}_j^{n+1}$. Then the parameters are updated as $\epsilon_j^{n+1}=\epsilon(\widetilde{W}_j^{n+1})$, $\kappa_j^{n+1}=\kappa(W_j^{n+1})$ and $C_{vt,j}^{n+1}=C_{vt}(W_j^{n+1})$ using (2.5), (2.11) and (2.15), respectively.

(ii). The temperature T_j^{n+1} is obtained from Eq. (3.4), where the calculation of $\Gamma_{s,j}^n$ will be given in next subsection.

(iii). The discrete vapor equation (3.5) is solved for the vapor concentration $C_{v,j}^{n+1}$.

(iv). Finally, the discrete pressure equation (3.6) is solved to obtain P_j^{n+1} and the total mixture gas concentration is calculated by $C_j^{n+1}=P_j^{n+1}/(RT_j^{n+1})$. The air concentration is updated by $C_{a,j}^{n+1}=C_j^{n+1}-C_{v,j}^{n+1}$.

At each time step, we only need to solve a tridiagonal linear system for each variable. Since the finite volume formulation is based on a discrete conservation form, our method

maintains the conservation of vapor and energy (heat flux). In the above discrete scheme, air equation (2.2) is replaced with the pressure equation (3.1). Nevertheless, conservation of air mass is also maintained discretely. In order to see this, we add the discrete vapor and pressure equations, respectively, from $j=2$ to $N-1$ to get

$$\sum_{j=2}^{N-1}\Delta x\left(\frac{\epsilon_j^{n+1}P_j^{n+1}}{RT_j^{n+1}\Delta t}-\frac{\epsilon_j^nP_j^n}{RT_j^n\Delta t}\right)=\frac{1}{(\Delta x)}\left[V_{G,N-1/2}\frac{\epsilon_{N-1/2}^nP_{N-1/2}^n}{RT_{N-1/2}^n}\delta_xP_N^{n+1}\right.$$
$$\left.-V_{G,3/2}\frac{\epsilon_{3/2}^nP_{3/2}^n}{RT_{3/2}^n}\delta_xP_2^{n+1}\right]-\sum_{j=2}^{N-1}(\beta_GS_{1,j}^{n+1}+\Gamma_{s,j}^n),\tag{3.19}$$

and

$$\sum_{j=2}^{N-1}\Delta x\frac{\epsilon_j^{n+1}C_{v,j}^{n+1}-\epsilon_j^nC_{v,j}^n}{\Delta t}=\frac{1}{2(\Delta x)}\left[V_{G,N-1/2}\epsilon_{N-1/2}^nC_{v,N-1/2}^{n+1}\delta_xP_N^n\right.$$
$$\left.-V_{G,3/2}\epsilon_{3/2}^nC_{v,3/2}^{n+1}\delta_xP_2^n\right]+\frac{\delta_G}{\Delta x}\left[\epsilon_{N-1/2}^nC_{N-1/2}^n\delta_x\left(C_{v,N}^{n+1}/C_N^n\right)\right.$$
$$\left.-\epsilon_{3/2}^nC_{3/2}^n\delta_x\left(C_{v,2}^{n+1}/C_2^n\right)\right]-\sum_{j=2}^{N-1}(\beta_GS_{1,j}^{n+1}+\Gamma_{s,j}^n).\tag{3.20}$$

By combining boundary conditions with the above equations, we have

$$\frac{\Delta x}{2}\left(\frac{\epsilon_1^{n+1}P_1^{n+1}}{RT_1^{n+1}\Delta t}-\frac{\epsilon_1^nP_1^n}{RT_1^n\Delta t}\right)+\frac{\Delta x}{2}\left(\frac{\epsilon_N^{n+1}P_N^{n+1}}{RT_N^{n+1}\Delta t}-\frac{\epsilon_N^nP_N^n}{RT_N^n\Delta t}\right)+\sum_{j=2}^{N-1}\Delta x\left(\frac{\epsilon_j^{n+1}P_j^{n+1}}{RT_j^{n+1}\Delta t}-\frac{\epsilon_j^nP_j^n}{RT_j^n\Delta t}\right)$$
$$=\frac{C_v^o-C_{v,N}^{n+1}}{R_v^o+1/H_v^o}+\frac{C_a^o-C_{a,N}^n}{R_a^o+1/H_a^o}-\frac{C_{v,1}^{n+1}-C_v^i}{R_v^i+1/H_v^i}-\frac{C_{a,1}^n-C_a^i}{R_a^i+1/H_a^i}-\sum_{j=2}^{N-1}(\beta_GS_{1,j}^{n+1}+\Gamma_{s,j}^n),\tag{3.21}$$

$$\frac{\Delta x}{2}\frac{(\epsilon_1^{n+1}C_{v,1}^{n+1}-\epsilon_1^nC_{v,1}^n)}{\Delta t}+\frac{\Delta x}{2}\frac{(\epsilon_N^{n+1}C_{v,N}^{n+1}-\epsilon_N^nC_{v,N}^n)}{\Delta t}+\sum_{j=2}^{N-1}\Delta x\frac{(\epsilon_j^{n+1}C_{v,j}^{n+1}-\epsilon_j^nC_{v,j}^n)}{\Delta t}$$
$$=\frac{C_v^o-C_{v,N}^{n+1}}{R_v^o+1/H_v^o}-\frac{C_{v,1}^{n+1}-C_v^i}{R_v^i+1/H_v^i}-\sum_{j=2}^{N-1}(\beta_GS_{1,j}^{n+1}+\Gamma_{s,j}^n).\tag{3.22}$$

It follows that

$$\frac{\Delta x}{2}\frac{(\epsilon_1^{n+1}C_{a,1}^{n+1}-\epsilon_1^nC_{a,1}^n)}{\Delta t}+\frac{\Delta x}{2}\frac{(\epsilon_N^{n+1}C_{a,N}^{n+1}-\epsilon_N^nC_{a,N}^n)}{\Delta t}+\sum_{j=2}^{N-1}\Delta x\frac{(\epsilon_j^{n+1}C_{a,j}^{n+1}-\epsilon_j^nC_{a,j}^n)}{\Delta t}$$
$$=\frac{C_a^o-C_{a,N}^n}{R_a^o+1/H_a^o}-\frac{C_{a,1}^n-C_a^i}{R_a^i+1/H_a^i}.\tag{3.23}$$

The left-hand side of Eq. (3.23) represents a discrete form (trapezoidal formula) of the change in air mass. Hence the above equation validates that the rate of air mass change equals to the net air mass flux entering the clothing assembly.

3.2 Water absorption by fiber

We now turn our attention to the water absorption by fiber W_f and the source term Γ_s. The amount of the water absorbed by fibre C_f (mole per unit volume) satisfies Eq. (2.9) together with the initial and boundary conditions

$$C_f'(r,0)=0, \quad C_f'(R_f,t)=\frac{\rho W_f'(RH)}{M}, \quad \left.\frac{\partial C_f'}{\partial r}\right|_{r=0}=0, \tag{3.24}$$

where the relative humidity is related to the vapor content by $RH=C_vRT/P_{sat}(T)$. The water absorption by fibre can be rewritten by

$$W_f=\frac{2M}{\rho R_f^2}\int_0^{R_f} C_f' r dr=\frac{2W_f'(RH)}{R_f^2}\int_0^{R_f} C_f^{*'} r dr=W_f'(RH)C_f^*, \tag{3.25}$$

where

$$C_f^*=\frac{2}{R_f^2}\int_0^{R_f} C_f^{*'} r dr \tag{3.26}$$

and $C_f^{*'}$ denotes a scaled water absorption, which is the solution of the initial-boundary problem

$$\begin{aligned}&\frac{\partial C_f^{*'}}{\partial t}=\frac{1}{r}\frac{\partial}{\partial r}\left(D_f r\frac{\partial C_f^{*'}}{\partial r}\right), \quad 0\le r\le R_f, \ t>0, \\ &C_f^{*'}(r,0)=0, \quad \left.\frac{C_f^{*'}}{\partial r}\right|_{r=0}=0, \quad C_f^{*'}(R_f,t)=1.\end{aligned} \tag{3.27}$$

Since Eq. (3.27) is a linear evolution equation, we use the central finite difference with a uniform mesh on $[0,R_f]$. The finite difference system for the scaled water absorption is given by

$$\frac{C_{f,i}^{*',n+1}-C_{f,i}^{*',n}}{\Delta t}=\frac{D_f}{r_i(\Delta r)^2}\delta_x\left(r_{i+1/2}\delta_x C_{f,i+1}^{*',n+1}\right), \quad i=1,\cdots,M, \tag{3.28}$$

with

$$C_{f,i}^{*',0}=0, \quad C_{f,M}^{*',n+1}=1, \quad \frac{C_{f,2}^{*',n+1}-C_{f,1}^{*',n+1}}{\Delta r}=0, \tag{3.29}$$

where $r_i=i\Delta r$ and Δr denotes the stepsize in r-direction. From the scaled water content, we can calculate the water absorption by fiber by

$$W_f^{n+1}=W_f'(RH^n)C_f^{*,n+1}, \tag{3.30}$$

where $C_f^{*,n+1}$ can be calculated by a classical trapezoidal rule. Finally, the source term Γ_s can be calculated by

$$\begin{aligned}\Gamma_{s,j}^n &= (1-\epsilon')\frac{\partial C_f}{\partial t}\bigg|_{t=t_n} = (1-\epsilon')\frac{2D_f}{R_f}\frac{\partial C_f'}{\partial r}\bigg|_{r=R_f,t=t_n}\\ &= (1-\epsilon')\frac{2D_f\rho W_f'(RH_j^n)}{MR_f}\frac{\partial C_f^{*'}}{\partial r}\bigg|_{r=R_f,t=t_n}\\ &\approx (1-\epsilon')\frac{2D_f\rho W_f'(RH_j^n)}{MR_f}\frac{(C_{f,M}^{*',n}-C_{f,M-1}^{*',n})}{\Delta r}.\end{aligned} \tag{3.31}$$

At each time step of the above scheme, we only need to calculate the scaled water content $C_{f,i}^{*',n+1}$ which is independent of x_j. We plot the scaled water absorption $C_f^{*'}$ and C_f^* in Fig. 4, which shows that the diffusion of moisture in fibre is very slow.

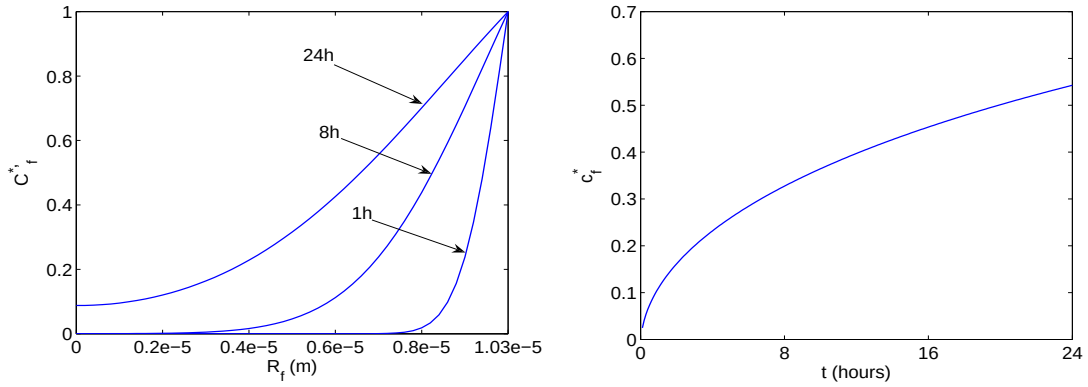

Figure 4: Scaled water absorption by fibre ($C_f^{*'}$ and C_f^*).

In the case of polyester batting, the maximum of water content absorbed by fiber is less than 2%. In this case, the water absorption by fibre can be neglected and $W \approx \widetilde{W}$. But in the case of viscose batting, fiber can absorb up to 29% water and the water absorption by fibre must be taken into account. The total water content is the sum of the water absorption by fibre and the water on the surface.

4 Numerical results and discussion

In this section, computational results are presented for the heat/moisture transfer in a clothing assembly with a porous batting sandwiched by two covering layers. Four cases are considered:

- Case I: 10-pile polyester batting with laminated cover;

Table 1: Physical parameters for cover materials.

Properties	laminated	Nylon
Thickness (m)	5.15E-4	2.73E-4
Density (kg/m^3)	4.27E+3	3.96E+3
Porosity	0.1	0.1
Thermal resistance (km^2/W)	3.16E-2 (R_T)	3.15E-2 (R_T)
Resistance to vapor (s/m)	143.79 (R_v)	64.99 (R_v)
Resistance to air penetration $(kPas/m)$	Impermeable (R_a)	0.524 (R_a)

Table 2: Physical parameters for batting materials.

parameter	polyester	viscose	unit
ρ in (2.5)	1.39×10^3	1.53×10^3	$\mathrm{kgm^{-3}}$
ϵ' in (2.5)	0.993	0.951	
D_f in (2.9)	non-hygroscopic	1.0×10^{-16}	$\mathrm{m^2s^{-1}}$
E in (2.7)	2.4×10^{-6}	2.4×10^{-6}	
κ_f in (2.11)	1×10^{-1}	1.5×10^{-1}	$\mathrm{Wm^{-1}K^{-1}}$
C_{vf} in (2.15)	1.17×10^6	1.3×10^6	$\mathrm{Jm^{-1}K^{-1}}$
L	$4.92\times10^{-3}\times10$	1×10^{-4}	m
R_f	1.03×10^{-5}	1.03×10^{-5}	m

- Case II: 10-pile polyester batting with nylon cover;
- Case III: 15-pile viscose batting with laminated cover;
- Case IV: 15-pile viscose batting with nylon cover.

Physical parameter values are presented in Table 1 for the cover materials and in Table 2 for the batting materials. Other parameter values can be found in [5, 11]. The resistances to air and vapor are different for each material and the laminated cover is impermeable for air. Each individual case was investigated in [4, 5, 11], respectively, with different mathematical models and finite difference methods. Experimental measurements for water accumulated in the cloth assembly were given in [6]. To compare with the experimental measurements, we take $H_v^i = H_a^i = H_t^i = 0$ as in [6]. Here all numerical results are obtained using the finite volume method with $\Delta t = 10s$, $\Delta x = L/100$ (1% of the batting length) and $\Delta r = R_f/50$. Tests with various spatial and temporary step sizes have been carried out to ensure the convergence of our numerical results. All computations were performed on a Blade 1000 Sun-workstation in complex double precision.

For case I, we present in Fig. 5 numerical results for vapor concentration C_v, air concentration C_a, temperature T, source distribution S_1 and total water content W at 8 and 24 hours, respectively. The comparison between numerical results and experimental measurements [6] on accumulated water content for cases II–IV is presented in Figs. 6-8. Several observations are in order:

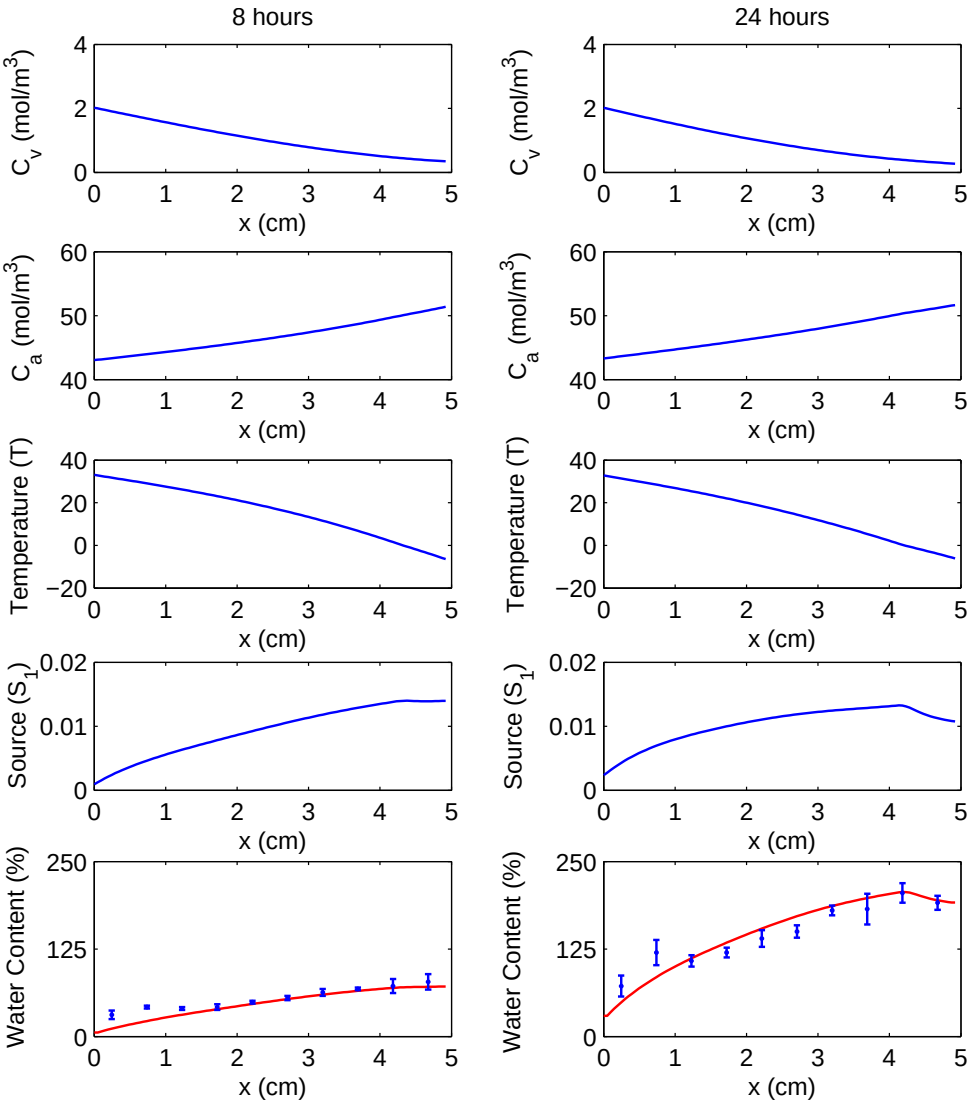

Figure 5: Numerical results for 10 piles polyester batting sandwiched by two layers of laminated fabric.

• We have used a splitting approach and a semi-implicit scheme for each equation. The semi-implicit scheme usually is conditionally stable. Our numerical experiments show that the scheme is stable when the time-step is smaller than 20 seconds, which is much less restrictive than ones used in [5,11].

• In all cases, vapor concentration and temperature are monotonically decreasing from the inner cover to the outer cover while air concentration is increasing. This confirms that the air flow provides an extra resistance to the vapor flux.

• Physically there is an interface between the wet and frozen zones since the conductivity, capacity and latent heat have a jump across the interface. Since the amount of

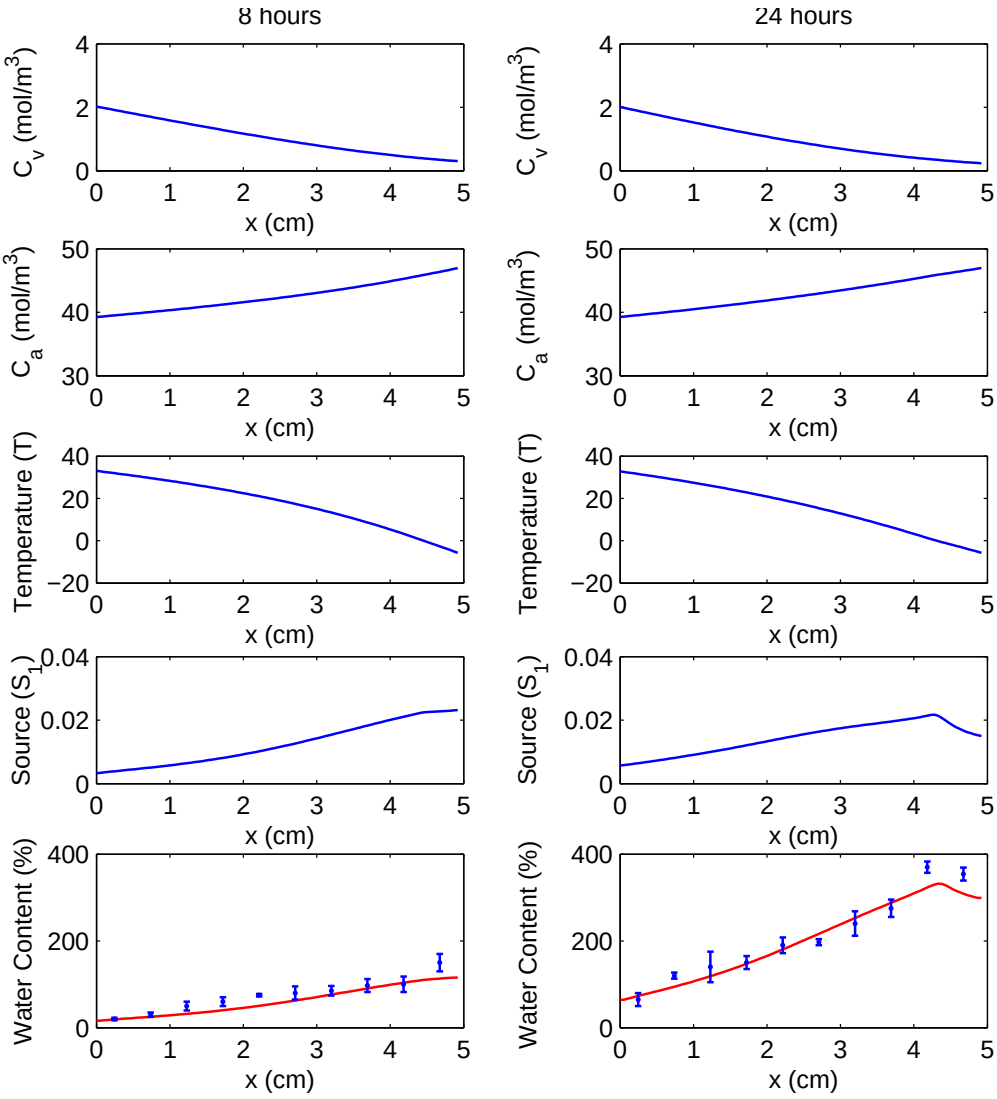

Figure 6: Numerical results for 10 piles polyester batting sandwiched by two layers of nylon fabric.

water is not very large, the discontinuity for vapor, air and temperature is not apparent. The discontinuity for source term can be observed from Figs. 5, 6 and 8 at approximately 1/5 length of the batting from outer cover where $T \approx 0$. Numerical solutions near this interface may be not very accurate. To obtain better accuracy, special treatments such as IIM or local refinement techniques [15, 18, 24], may be needed.

• Our numerical experiments show that vapor concentration C_v, air concentration C_a and temperature T reach the steady state at approximately the 20 minute mark. The source profile reach the steady-state in at a much later time (several hours) since it is very sensitive to the vapor concentration and the temperature. The spatial water con-

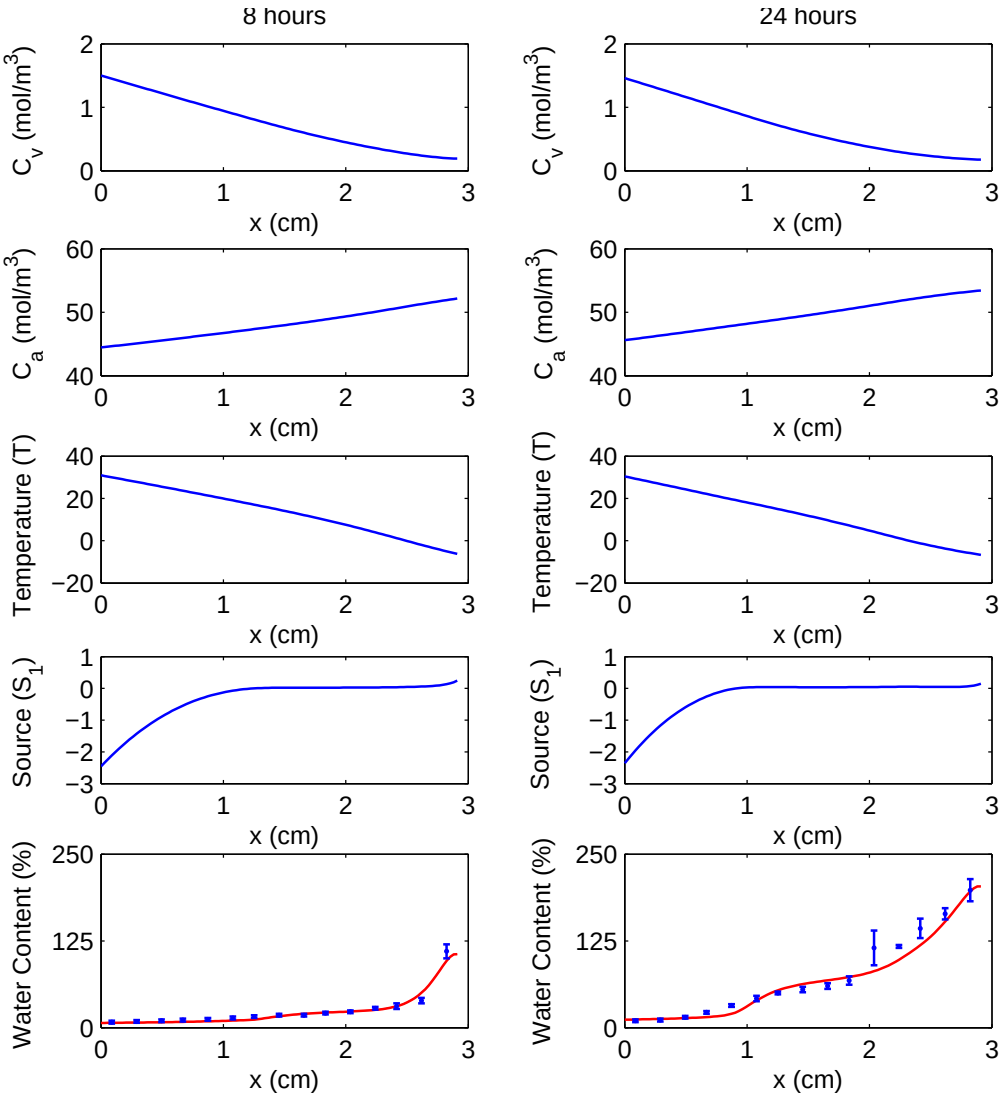

Figure 7: Numerical results for 15 piles viscose batting sandwiched by two layers of laminated fabric.

tent variation resembles that of the source profile. This shows the possibility to simplify this physical process into a quasi-steady state model, in which one only needs to calculate steady-state solutions of vapor and air concentrations and temperature while liquid water accumulation can be approximated by taking the steady-state solutions and integrating the water equation in time.

• In all cases, numerical results of the water content are in good agreement with experimental data. We can see from Figs. 5, 6 and 8 that water content is increasing in the wet zone and decreasing in the frozen zone. It is interesting to note that the profound decrease in the accumulated water content predicted by our model agrees with the ex-

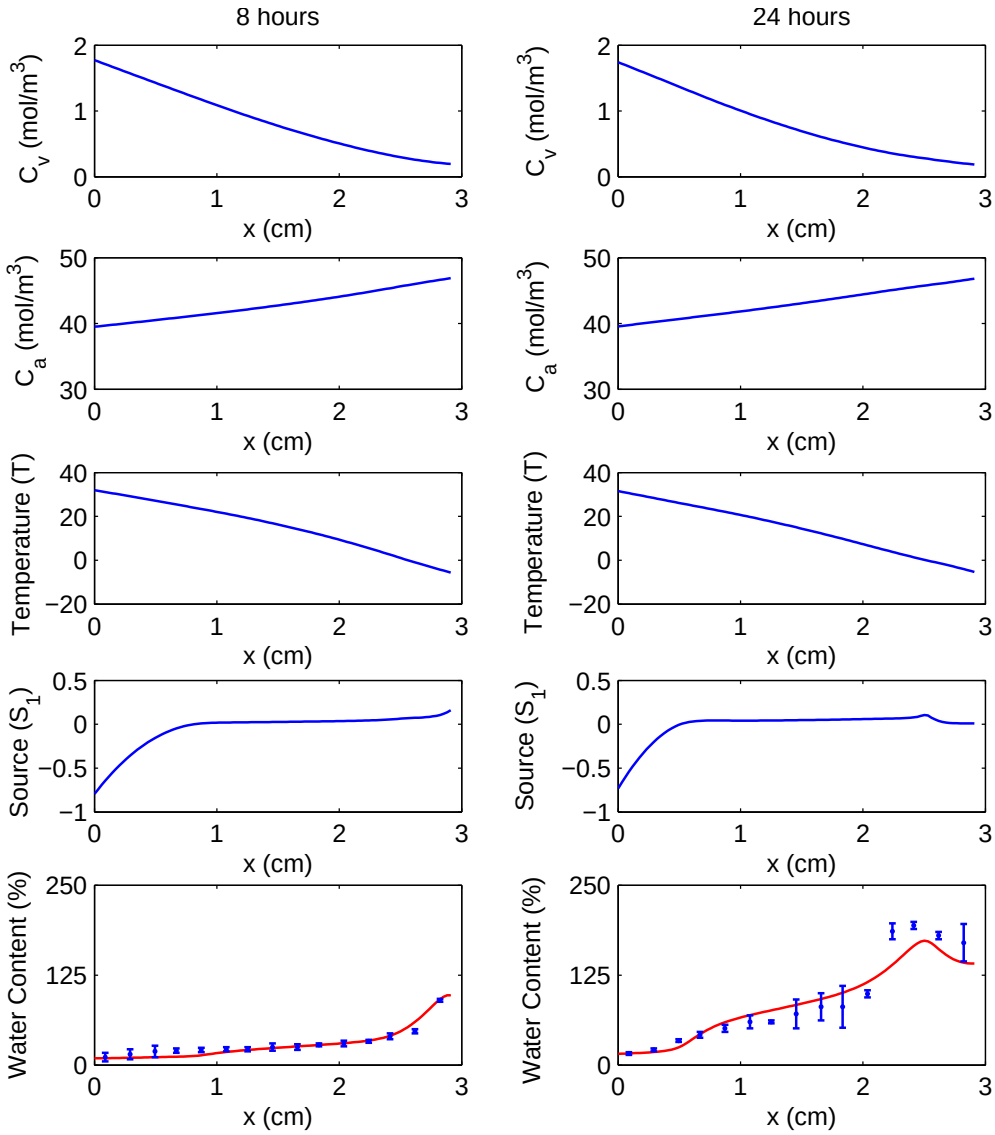

Figure 8: Numerical results for 15 piles viscose batting sandwiched by two layers of nylon fabric.

perimental results, contrary to the numerical results from previous models [3, 5]. Since nylon fabric is more permeable to air and vapor movement, it allows more influx of vapor from the inner boundary (artificial skin). Our numerical results show that the overall water accumulation for the assemblies with nylon cover is more than that with laminated cover. Compared numerical results in Figs. 5 and 6 and in Figs. 7 and 8 (different batting materials), we can see that the source for viscose batting is negative (evaporation) near the inner boundary while the source for the polyester batting is always positive (condensation). Also water content for viscose batting seems to increase more rapidly from

the wet zone to the frozen zone than that for polyester batting. This indicates that the assemblies with viscose batting may push more water to the right boundary of clothing assemblies and keep the inner boundary region (human skin) dry. It can also be seen that vapor concentration for 10 piles polyester batting is always larger than that for 15 piles viscose batting, possibly due to different porosity values.

5 Conclusions

We have presented a numerical study of moisture transport in textile materials by a finite volume method. Compared with previous models in [5,11], the water equation has been simplified by omitting the convection and capillary effects since the volume fraction of water is relatively small. A more realistic formula for heat conductivity and heat capacity is proposed. Numerical results show that the current model is more realistic than the previous ones reported in the literature. Compared with the finite difference methods used in previous studies [4,5,11], the finite volume method presented in this paper has certain advantages as it maintains the discrete conservation for all these physical components and provides a more accurate physical representation of the heat and liquid moisture transfer. Also the method is helpful in better dealing with the boundary of dramatic change especially in the fibrous combinations of multiple types of fibrous battings. Furthermore, the splitting scheme proposed in this paper is very efficient, therefore is more suitable for the type of problems studied here due to the relative long time horizons associated with experiments. This becomes particularly important when we apply our model to multi-dimensional problems.

Acknowledgments

The research of Ye and Sun was supported in part by a grant from CityU (7001926). The research of Huang is supported by the Natural Science and Engineering Council (NSERC) and the Mathematics of Information Technology and Complex Systems (MITACS) of Canada. The research of Fan is supported by Hong Kong Polytechnic University (Project No. G-U165).

References

[1] M.K. Choudhary, K.C. Karki, and S.V. Patankar, Mathematical modeling of heat transfer, condensation, and cappilary flow in porous insulation on a cold pipe. *Int. J. Heat Mass Transfer* 47 (2004), pp. 5629-5638.

[2] H.G. David, P. Nordon, Case studies of coupled heat and moisture diffusion in wool beds, *Textile Res. J.* 39 (1939) pp. 166-172

[3] J. Fan, Z. Luo and Y. Li, Heat and moisture transfer with sorption and condensation in porous clothing assemblies and numerical simulation, *Int. J. Heat Mass Transfer*, 43 (2000), pp. 2989-3000.

[4] J. Fan and X. Wen, Modelling heat and moisture transfer, *Int. J. Heat Mass Transfer*, 45 (2002), pp. 4045-4055.
[5] J. Fan, X. Cheng, X. Wen and W. Sun, An improved model of heat and moisture transfer with phase change and mobile condensates in fibrous insulation and comparison with experimental results, *Int. J. Heat Mass Transfer*, 47 (2004), pp. 2343-2352.
[6] J. Fan, X. Cheng and Y.-S. Chen, An experimental investigation of moisture absoption and condensation in fibrous insulations under low temperature, *Experimental Thermal and Fluid Science*, 27 (2003), pp. 723-729.
[7] W.R. Foss, C.A. Bronkhorst, and K.A. Bennett, Simultaneous heat and mositure transport in paper sheets during moisture sorption from humid air, *Int. J. Heat Mass Transfer* 46 (2002), pp. 2875-2886.
[8] J. Geiser. Discretization methods with analytical solutions for convection-diffusion-dispersion-reaction-equations and application. *J. Eng. Math.*, 57 (2007), pp. 7998.
[9] P.S.H. Henry, Diffusion in Absorbing media, *Proc. Roy. Soc.* 171A (1939), pp. 215-241.
[10] P.S.H. Henry, Diffusion of moisture and heat through textiles, *Discuss. Faraday Soc.*, 3 (1948), pp. 243-257.
[11] H. Huang, C. Ye and W. Sun, Moisture transport in fibrous clothing assemblies, *J. Eng. Math.*, (2008), in press.
[12] W. Hundsdorfer and J.G. Verwer, *Numerical Solution of Time-Dependent Advection-Diffusion-Reaction Equations*, Springer, Berlin, 2003.
[13] F.E. Jones, *Evaporation of Water*, Lewis Publishers Inc., Michigan, 1992, pp. 25-43.
[14] S. Kumar, N. Nataraj and A. Pani, Finite volume element method for second order hyperbolic equations, *Int. J. Numerical Analysis & Modeling*, 5(2008), pp.132–151.
[15] R.J. LeVeque and Z. Li, The immersed interface method for elliptic equations with discontinuous coefficients and singular sources, *SIAM J. Numer. Anal.*, 31(1994), pp. 1019-1044.
[16] R.J. LeVeque, Finite Volume Methods for Hyperbolic Problems, Cambridge Texts in Applied Mathematics, Cambridge University Press, 2002.
[17] Y. Li, and B.V. Holcombe, A two-stage sorption model of the coupled diffusion of moisture and heat in wool fabric, *Textile Res. J.* 62 (1992), pp. 211-217
[18] T. Lin, Y. Lin and W. Sun, Error estimation of a class of quadratic immersed finite element methods for elliptic interface equations, *Discrete Contin. Dyn. Syst. Ser. B*, 7(2007), pp. 807–823.
[19] Y. Ogniewicz and C.L. Tien, Analysis of condensation in porous insulation, *J. Heat Mass Transfer*, 24 (1981), pp. 421-429.
[20] A.P. Shapiro and S.Motakef, Unsteady heat and mass transfer with phase change in porous slab: analytical solutions and experimental results, *J. Heat Mass Transfer*, 33 (1990), pp. 163-173.
[21] P. Smith and E.T. Twizell, A transient model of thermoregulation in a clothed human, *Applied Math. Modeling*, 8 (1984), pp. 211-216.
[22] R. Taylor and R. Krishna, *Multicomponent Mass Transfer*, John Wiley & Sons Inc., New York, 1993, pp. 50-66.
[23] J.W. Thomas, Numerical Partial Differential Equations: Finite Difference Mehods, Springer, 1995.
[24] H. Wang, An improved WPE method for solving discontinuous Fokker-Planck equations, *Int. J. Numerical Analysis & Modeling*, 5(2008), pp.1–23.